



e-ISSN: 2319-8753 | p-ISSN: 2347-6710

IJIRSET

International Journal of Innovative Research in
SCIENCE | ENGINEERING | TECHNOLOGY

INTERNATIONAL JOURNAL OF INNOVATIVE RESEARCH

IN SCIENCE | ENGINEERING | TECHNOLOGY

Volume 11, Issue 1, January 2022

ISSN INTERNATIONAL
STANDARD
SERIAL
NUMBER
INDIA

Impact Factor: 7.569

9940 572 462

6381 907 438

ijirset@gmail.com

www.ijirset.com



Optimization of AC Load Linearization Process and Fixing OPF Problems Using QC and SOC Combined Structure

Ehsan Yousefi Nejad¹

Department of Electrical Engineering, Semnan University, Semnan, Iran¹

ABSTRACT: With the increase of injection of scattered products in the power network, attention to this level of products in the load distribution of the power system has also increased. In this chapter, it is assumed that the values of scattered source output or the active and reactive power consumed by the system are AC and numerical and point-to-point values are not available for these input variables. However, in this chapter, real data has been used to model the AC model to model the distributed generation source. In this section, with the aim of estimating the AC model, the voltage range and angles of the power system buses, the active and reactive powers passing through the lines and the reactive power produced by the PV buses, the AC load distribution method has been used. In this method, linearization of nonlinear load distribution equations is used to find the output variables of the problem.

KEYWORDS: nonlinear load distribution, AC model, active and reactive power, scattered source output.

I. INTRODUCTION

Load distribution analysis is one of the most important aspects of operation and planning in the power system. In definite load distribution, all powers injected into the power system and network topology are considered as specific values. This is in the context that system mode variables are random in nature due to random changes in load and scattered output, inaccurate estimation of system load and network parameters. By taking into account the uncertainties in the load and the output of the power system, it is possible to improve the load distribution that is done as usual. Possible load distribution in the power grid is divided into three general categories: numerical, analytical and approximate methods. In probabilistic load distribution, random variables are considered as probabilistic distribution functions. Of course, some researchers model random variables in the power system as random processes and use sequential Monte Carlo methods to solve the problem and consider the temporal correlation between the variables. In modelling the load and output of the power system, the changes of each variable must be properly simulated separately, the probabilistic distribution function, and the relationship between the load and the output of the system. Conventional methods for modelling the relationship between variables include the independence of variables, linear relationship between variables, and other complex methods. The use of analysis in simulating power system parameters is gradually increasing. On the other hand, due to the increase of distributed generation units in the power grid and the knowledge of the time dependence between distributed distribution and system load, AC can be used to analyse the load distribution in the power system. Once performed, a definite load distribution cannot check all possible operating points in a system. In previous studies, the load and output of the system have been used sequentially and sequentially, by distributing consecutive loads. By having information about system variables over a period of time or model simulation, the relationship between load variables and system output will be easily modelled. But using this method requires playing multiple loads. For example, if the load is distributed on an hourly basis, we will need 8760 loads per year.

II. PROPOSED LOAD DISTRIBUTION METHOD

The proposed method uses linearization of all nonlinear parts in the load distribution equations. In fact, this method is a continuation of the methods of formulations 1, 2 and 3. In this method, to find the points around which linearization takes place, it averages a definite load distribution around the points. In a definite load distribution, the values known in the equation include the active injection power in all buses except the slack bus, the reactive injection power in all PQ buses, and the voltage range in all bus generators.

Load distribution equations can be written in general equations 1 to 5.



$$P_i = V_i \sum_{k=1}^n V_k (G_{ik} \cos \theta_{ik} + B_{ik} \sin \theta_{ik}) \quad (1)$$

$$Q_i = V_i \sum_{k=1}^n V_k (G_{ik} \sin \theta_{ik} - B_{ik} \cos \theta_{ik}) \quad (2)$$

Where $i = 1, 2, \dots, n$.

$$P_{ik} = -t_{ik} G_{ik} V_i^2 + V_i V_k (G_{ik} \cos \theta_{ik} + B_{ik} \sin \theta_{ik}) \quad (3)$$

$$Q_{ik} = t_{ik} B_{ik} V_i^2 - B_{ik}' V_i^2 + V_i V_k (G_{ik} \sin \theta_{ik} - B_{ik} \cos \theta_{ik}) \quad (4)$$

$$Q_{i(sh)} = V_i^2 B_{i(sh)} \quad (5)$$

where in:

B_{ik} : The imaginary part of the ik element of the admittance matrix

$B_{i(sh)}$: The imaginary part of parallel admittance on the bus i

$\frac{1}{2} B_{ik}$: half of the ik line susceptance

G_{ik} : The real part of the ik element of the admittance matrix

n : Number of buses

P_i : Injectable active power in the bus i

P_{ik} : Active power across line $i-k$

Q_i : Injectable reactive power at bus i

Q_{ik} : Reactive power across line $i-k$

$Q_{i(sh)}$: Reactive power injected by a parallel element in the bus i

t_{ik} : Tap transform ratio

V_i : Voltage range at bus i

θ_{ik} : The difference in angles between the buses i and k .

In convolution technique based on analytical load distribution methods, an attempt is made to convert nonlinear equations 3 to 3 into equations that contain only the sum or difference of independent random variables. Finally, use the convolution technique to find the density functions of unknown problem variables. But this chapter uses this linearization of equations in a different way. In the linearization of load distribution equations in Formulation 4, unlike the previously proposed methods, the relationship between active and reactive powers is considered, which will have a significant effect on improving the voltage responses and reactive power of the lines.

First, to determine the linearization steps in this method, we consider two random variables X and Y , which are multiplied together to create a new random variable Z :

$$Z = XY \quad (6)$$

Now if the mean values of the random variables X and Y are X_0 and Y_0 , respectively, and ΔX and ΔY show the changes of these variables around the mean point:

$$X = X_0 + \Delta X \quad (7)$$

$$Y = Y_0 + \Delta Y \quad (8)$$

$$\begin{aligned} Z &= (X_0 + \Delta X)(Y_0 + \Delta Y) \approx X_0 Y_0 + X_0 \Delta Y + Y_0 \Delta X \\ &= X_0 Y_0 + Y_0 \Delta X + X_0 \Delta Y \quad (9) \end{aligned}$$

Now this technique can be used to linearize the angles and voltages of the power system due to the small change in random variables.

According to Equations 37 to 39 for Equations 10 and 11, linearization is performed:

$$V_i V_k = V_{i0} V_k + V_{k0} V_i - V_{i0} V_{k0} \quad (10)$$



$$V_i^2 = 2V_{i0}V_i - V_{i0}^2 \quad (11)$$

We will also have equations 12 and 13 for the McLaren series:

$$(12) \sin \theta_{ik} \approx \theta_{ik} - \frac{\theta_{ik}^3}{6}$$

$$\cos \theta_{ik} \approx 1 - \frac{\theta_{ik}^2}{2} \quad (13)$$

By applying equations 6 to 9 to linearize the expressions 12 and 13 we will have:

$$\cos \theta_{ik} = a_{ik} + b_{ik}\theta_{ik} \quad (14)$$

$$(15) \quad \sin \theta_{ik} = c_{ik} + d_{ik}\theta_{ik}$$

where $a_{ik} = 1 + \frac{\theta_{ik0}^2}{2}$, $b_{ik} = -\theta_{ik0}$, $c_{ik} = \frac{\theta_{ik0}^3}{3}$, $d_{ik} = 1 - \frac{\theta_{ik0}^2}{2}$

As can be seen in Equations 10 and 11, as well as 14 and 15, linearization has been performed for the angles and voltages of the system around the mean point.

However, according to the nonlinear load distribution equations, in this method, the expressions $V_i V_k \cos \theta_{ik}$, $V_i V_k \sin \theta_{ik}$ must also be linearized, which we will have according to the relations 10, 14 and 15:

$$V_i V_k \sin \theta_{ik} = a_{ik}' + b_{ik}'\theta_{ik} + c_{ik}'V_i + d_{ik}'V_k \quad (16)$$

$$V_i V_k \cos \theta_{ik} = a_{ik}'' + b_{ik}''\theta_{ik} + c_{ik}''V_i + d_{ik}''V_k \quad (17)$$

that

$$a_{ik}' = 2V_{i0}V_{k0}(\frac{1}{3}\theta_{ik0}^2 - 1)$$

$$b_{ik}' = V_{i0}V_{k0}(1 - \frac{1}{2}\theta_{ik0}^2)$$

$$c_{ik}' = V_{k0}(\theta_{ik0} - \frac{1}{6}\theta_{ik0}^3)$$

$$d_{ik}' = V_{i0}(\theta_{ik0} - \frac{1}{6}\theta_{ik0}^3)$$

$$a_{ik}'' = V_{i0}V_{k0}(\frac{3}{2}\theta_{ik0}^2 - 1)$$

$$b_{ik}'' = -V_{i0}V_{k0}\theta_{ik0}$$

$$c_{ik}'' = V_{k0}(1 - \frac{1}{2}\theta_{ik0}^2)$$

$$d_{ik}'' = V_{i0}(1 - \frac{1}{2}\theta_{ik0}^2)$$

The equation of active power injected into the buses can be written as follows:

$$P_i = \sum_{k=1}^n f_{ik}'\theta_i - f_{ik}'\theta_k + g_{ik}'V_i + h_{ik}'V_k + e_{ik}' \quad (18)$$

where in:

$$e_{ik}' = a_{ik}''G_{ik} + a_{ik}'B_{ik}$$

$$f_{ik}' = b_{ik}''G_{ik} + b_{ik}'B_{ik}$$

$$g_{ik}' = c_{ik}''G_{ik} + c_{ik}'B_{ik}$$

$$h_{ik}' = d_{ik}''G_{ik} + d_{ik}'B_{ik}$$

Equation 18 can also be changed to form 19:



$$P_i = \sum_{k=1 \neq i}^n (-f_{ik}' \theta_k) + \sum_{k=1 \neq i}^n f_{ik}' \theta_i + \sum_{k=1 \neq i}^n h_{ik}' V_k + \left(h_{ii}' + \sum_{k=1}^n g_{ik}' \right) V_i + \sum_{k=1}^n e_{ik}' \quad (19)$$

A similar equation to the form of Equation 19 can also be found for the reactive power injected into the system buses. Finally, the equations obtained for P_i and Q_i can be written in the following matrix form:

$$\begin{bmatrix} P \\ Q \end{bmatrix} = \begin{bmatrix} M' & L' \\ N' & J' \end{bmatrix} \begin{bmatrix} \theta \\ V \end{bmatrix} + \begin{bmatrix} R' \\ H' \end{bmatrix} \quad (20)$$

Where each of the variables P and Q contains n components. Equation 3-20 can also be written by changing the general form of Equation 21:

$$\begin{bmatrix} S_l \\ S_g \end{bmatrix} = \begin{bmatrix} M'' & L'' \\ N'' & J'' \end{bmatrix} \begin{bmatrix} X_l \\ X_g \end{bmatrix} + \begin{bmatrix} W_l' \\ W_g' \end{bmatrix} \quad (21)$$

where in:

$$S_l = \begin{bmatrix} P \\ Q_l \end{bmatrix}, S_g = \begin{bmatrix} Q_g \\ P_s \end{bmatrix}, X_l = \begin{bmatrix} \theta \\ V_l \end{bmatrix}, X_g = \begin{bmatrix} V_g \\ \theta_s \end{bmatrix} \quad (22)$$

The vectors P and θ above include all buses except the slack bus, P_l and Q_l include the PQ, Q_g and V_g buses including all PV buses and P_s and θ_s include the slack bus.

Formulation of the proposed method

Common analytical load distribution methods are based on mathematical calculations and the use of convolution techniques. In these methods, the function of distributing variables as input and the function of distributing system mode variables and power passing through lines is also the output of this method. One of the most important problems of this method is modeling the relationship between variables in different buses. In the proposed method, the aim is to find the proposed multivariate model for system mode variables including voltage and phase amplitude and power passing through network lines. That is why the formulation method introduced is used. This method linearizes the load distribution equations around the mean points and considers the relationship between active and reactive power. Previously, linearization of the proposed method was used to calculate the probabilistic distribution function of system state variables. But in this chapter, considering the proposed model, this method is used in a different way. In this method, the proposed model of load and system products and their placement in load distribution equations are used directly. In this method, it is assumed that the input injection powers to the system buses are given in the form of proposed models, that is, the active injection powers in PV busbars and the active and reactive injection powers in PQ busbars are available as proposed models. Also here, the amplitude and angle inputs of the slack bus as well as the voltage range of PV buses are considered as a fixed number, which can be interpreted as the existence of regulators that keep the busbar voltage constant. After inserting the proposed input models, the proposed multivariate output models including amplitude and phase voltage, reactive power injected into the PV bus, and line-passing powers can be obtained. To find the proposed model of amplitude and voltage phase, Equation 21 can be written as follows:

$$\begin{bmatrix} P \\ Q_l \end{bmatrix} = M'' \begin{bmatrix} \theta \\ V_l \end{bmatrix} + L'' \begin{bmatrix} V_g \\ \theta_s \end{bmatrix} + W_l' \quad (23)$$

According to the hypotheses above and the stability of some parameters, it can be concluded that the expression $L'' \begin{bmatrix} V_g \\ \theta_s \end{bmatrix}$ is a fixed vector and we have the following equation:

$$\begin{bmatrix} P \\ Q_l \end{bmatrix} = M'' \begin{bmatrix} \theta \\ V_l \end{bmatrix} + (L'' X_g + W_l') \quad (24)$$

Since equation 23 is established between the variables of the equation both at time t and at times t-1 and t-2, then equation 23 can be used this time with indices t and t-1 as 24 and 25 rewrite:

$$\begin{bmatrix} P_t \\ Q_{lt} \end{bmatrix} = M'' \begin{bmatrix} \theta_t \\ V_{lt} \end{bmatrix} + (L'' X_g + W_l') \quad (25)$$

$$\begin{bmatrix} P_{t-1} \\ Q_{lt-1} \end{bmatrix} = M'' \begin{bmatrix} \theta_{t-1} \\ V_{lt-1} \end{bmatrix} + (L'' X_g + W_l') \quad (26)$$

Equation 24 can now be written as Equation 26 to find the output variables $\begin{bmatrix} \theta_t \\ V_{lt} \end{bmatrix}$:



$$\begin{bmatrix} \theta_t \\ V_{lt} \end{bmatrix} = M''^{-1} \begin{bmatrix} P_t \\ Q_{lt} \end{bmatrix} + M''^{-1}(-L''X_g - W_l')(27)$$

As mentioned earlier, since all the active and reactive power of the known buses are assumed to be AC, the input can be represented as a matrix and multivariate of Equation 27:

$$\begin{bmatrix} P_t \\ Q_{lt} \end{bmatrix} = F_1 \begin{bmatrix} P_{t-1} \\ Q_{lt-1} \end{bmatrix} + F_2 \begin{bmatrix} P_{t-2} \\ Q_{lt-2} \end{bmatrix} + \dots + F_n \begin{bmatrix} P_{t-n} \\ Q_{lt-n} \end{bmatrix} + G_0 \begin{bmatrix} \epsilon_{Pt} \\ \epsilon_{Qlt} \end{bmatrix} + G_1 \begin{bmatrix} \epsilon_{Pt-1} \\ \epsilon_{Qlt-1} \end{bmatrix} + \dots + G_m \begin{bmatrix} \epsilon_{Pt-m} \\ \epsilon_{Qlt-m} \end{bmatrix} + C_0(28)$$

where in

C_0: AC constant component vector,

F_1 to F_n: The coefficient matrix for the moments t-1 to t-n are in the variable S_1,

n: is the maximum amount of time delay in the input coefficients,

G_0 to G_m: The matrix of MA coefficients for moments t to t-m for the Gaussian noise variable,

m: The maximum amount of time delay in the coefficients is the input AC.

Now by placing relation 27 in relation 26 we will have:

$$\begin{bmatrix} \theta_t \\ V_{lt} \end{bmatrix} = M''^{-1}F_1 \begin{bmatrix} P_{t-1} \\ Q_{lt-1} \end{bmatrix} + M''^{-1}F_2 \begin{bmatrix} P_{t-2} \\ Q_{lt-2} \end{bmatrix} + \dots + M''^{-1}F_n \begin{bmatrix} P_{t-n} \\ Q_{lt-n} \end{bmatrix} + M''^{-1}G_0 \begin{bmatrix} \epsilon_{Pt} \\ \epsilon_{Qlt} \end{bmatrix} + M''^{-1}G_1 \begin{bmatrix} \epsilon_{Pt-1} \\ \epsilon_{Qlt-1} \end{bmatrix} + \dots + M''^{-1}G_m \begin{bmatrix} \epsilon_{Pt-m} \\ \epsilon_{Qlt-m} \end{bmatrix} + M''^{-1}C_0 + M''^{-1}(-L''X_g - W_l')(29)$$

Therefore, multivariate models are obtained according to Equation 28 for the voltage and phase amplitude state variables. But as it turns out, Equation 28 is not the conventional equation of multivariate models. Because the variables on the right side of the equation are not seen on the left side of the equation and the matrix of the voltage and phase amplitude variables is not seen at the time of successive delays in this equation. To solve this problem, the following method is used to find the multivariate model coefficients according to Equations 24 and 25.

Since Equation 24 is valid for all moments t, t-1 and t-n. By placing relations 24, 25 and similar equations at consecutive latencies in Equation 28, we have:

$$\begin{bmatrix} \theta_t \\ V_{lt} \end{bmatrix} = M''^{-1}F_1 M'' \begin{bmatrix} \theta_{t-1} \\ V_{lt-1} \end{bmatrix} + M''^{-1}F_1(L''X_g + W_l') + M''^{-1}F_2 M'' \begin{bmatrix} \theta_{t-2} \\ V_{lt-2} \end{bmatrix} + M''^{-1}F_2(L''X_g + W_l') + \dots + M''^{-1}F_n M'' \begin{bmatrix} \theta_{t-n} \\ V_{lt-n} \end{bmatrix} + M''^{-1}F_n(L''X_g + W_l') + M''^{-1}G_0 \begin{bmatrix} \epsilon_{Pt} \\ \epsilon_{Qlt} \end{bmatrix} + M''^{-1}G_1 \begin{bmatrix} \epsilon_{Pt-1} \\ \epsilon_{Qlt-1} \end{bmatrix} + \dots + M''^{-1}G_m \begin{bmatrix} \epsilon_{Pt-m} \\ \epsilon_{Qlt-m} \end{bmatrix} + M''^{-1}C_0 + M''^{-1}(-L''X_g - W_l')(30)$$

Now if we define the final optimal model as Equation 30, which is a multivariate model for the output variables, we will have:

$$\begin{bmatrix} \theta_t \\ V_{lt} \end{bmatrix} = C_1 \begin{bmatrix} \theta_{t-1} \\ V_{lt-1} \end{bmatrix} + C_2 \begin{bmatrix} \theta_{t-2} \\ V_{lt-2} \end{bmatrix} + \dots + C_n \begin{bmatrix} \theta_{t-n} \\ V_{lt-n} \end{bmatrix} + E_0 \begin{bmatrix} \epsilon_{\theta t} \\ \epsilon_{V_{lt}} \end{bmatrix} + E_1 \begin{bmatrix} \epsilon_{\theta t-1} \\ \epsilon_{V_{lt-1}} \end{bmatrix} + \dots + E_m \begin{bmatrix} \epsilon_{\theta t-m} \\ \epsilon_{V_{lt-m}} \end{bmatrix} + C \quad (31)$$

By comparing Equation 29 with Equation 30, we can obtain the target model unknowns and we will have:

$$C_1 = M''^{-1}F_1 M''$$

$$C_2 = M''^{-1}F_2 M''$$

.

.

.

$$C_n = M''^{-1}F_n M''$$

$$C = M''^{-1}(C_0 + (-L''X_g - W_l')) + M''^{-1}(F_1 + F_2 + \dots + F_n)(L''X_g + W_l')(31)$$

But since the E_0 matrix in all models must be in the form of a single matrix, to find the variance of the noise component we need to use the rules for addition or subtraction of independent random variables. Using Equations 33 and 34, which are true for independent random variables in probability, the variance of the output random noise variable can be obtained:

$$Var(Y) = a^2 Var(X)$$

$$Var(X_1 \pm X_2) = Var(X_1) + Var(X_2)(32)$$

According to Equations 35 to 37, the output noise variance is equal to the quadratic of each of the H matrix elements multiplied by the input noise variance:



$$H = M^{-1}G_0$$

$$H \begin{bmatrix} \epsilon_{Pt} \\ \epsilon_{Qlt} \end{bmatrix} = E_0 \begin{bmatrix} \epsilon_{\theta t} \\ \epsilon_{Vlt} \end{bmatrix}$$

$$var \left(\begin{bmatrix} \epsilon_{\theta t} \\ \epsilon_{Vlt} \end{bmatrix} \right) = H.^{-2} var \left(\begin{bmatrix} \epsilon_{Pt} \\ \epsilon_{Qlt} \end{bmatrix} \right)$$

Similarly, we have the following equation for the matrix of coefficients E₁, E₂, ..., E_m:

$$E_1 = M^{-1}G_1ME_2 = M^{-1}G_2M \dots E_m = M^{-1}G_mM$$

III. NETWORK SIMULATION

In this section, the IEEE multi-bus network is selected to find the output variable model. The data of the studied system and network topology are presented in the appendix. Changes have been made in the study network to suit the type of problem. AC voltage and phase amplitude models are selected as output state variables and the method proposed in the previous section is used to find unknown coefficients in the model. The model of active and reactive loads on all network buses is assumed to be a simple model. The average values of the load model equal to the IEEE standard network data are selected. The model coefficients for all system loads are 0.3. Only the coefficient for injection power in bus number 2 is 0.2. The standard deviation values of the noise component are considered as a coefficient of the average values of active and reactive powers injected into the network. The variance for the injectable active and reactive power models is shown in Table 1 and 2. Also, according to the selection of the SOCP model to simulate the output power of the wind turbine and large changes in production power, the amount of 15 MW of injectable power has been considered as a constant for bus number 8.

Table 1: Random noise component variance for input injection powers

Injectable active and reactive power in different busses	Variance
(Active) 2	0.8372
(Active) 3	22.1841
(Active) 4	5.7121
(Reactive) 4	0.1521
(Active) 5	0.5776
(Reactive) 5	0.0256
(Active) 6	1.2544
(Active) 8	0.7661
(Active) 9	8.7025
(Reactive) 9	2.7556
(Active) 10	0.8100
(Reactive) 10	0.3364
(Active) 11	0.1225
(Reactive) 11	0.0324
(Active) 12	0.3721
(Reactive) 12	0.0256
(Active) 13	1.8225
(Reactive) 13	0.3364
(Active) 14	2.2201
(Reactive) 14	0.2500

Assuming the existence of active and reactive power injection models in network buses and according to the proposed method, a multivariate model can be obtained for network mode variables including amplitude and voltage phase. This method requires linearization of load distribution equations around mean points. These average points are obtained by a Newton-Raphson load distribution for average values of active and reactive power in network buses. For bus No. 8,



where the injection power has changed from the IEEE standard network, the average active injection power is considered as the sum of a constant power of 15 MW and the average wind turbine power output of 3,948 MW.

Table 2: Stability and variance of the random time output noise component

Variables	Fixed component	Noise variance
θ_2	-0.06369	0.0932
θ_3	-0.1468	0.6948
θ_4	-0.1248	0.3067
θ_5	-0.1043	0.2208
θ_6	-0.1470	0.6369
θ_7	-0.1385	0.6273
θ_8	-0.1173	0.6946
θ_9	-0.1626	0.8484
θ_{10}	-0.1633	0.8243
θ_{11}	-0.1573	0.7188
θ_{12}	-0.1566	0.7311
θ_{13}	-0.1593	0.7720
θ_{14}	-0.1713	0.9786
$ V_4 $	0.7546	0.0080
$ V_5 $	0.7462	0.0060
$ V_7 $	0.8852	0.0129
$ V_9 $	0.8261	0.0429
$ V_{10} $	0.8080	0.0363
$ V_{11} $	0.7771	0.0106
$ V_{12} $	0.7451	0.0051
$ V_{13} $	0.7483	0.0095
$ V_{14} $	0.7807	0.0504

The coefficient matrix for the first and twelfth time delay components is also shown in the following tables. In the display of these matrices, very small coefficients are omitted and these coefficients are considered zero.

Finally, the following method is used to check the correctness of the answers and models presented in the output. Output models can be simulated for amplitude and voltage phase variables. Input models of active and reactive power injected into the network can also be simulated, and input data can be used to find the point-to-point output of the amplitude and phase voltages by Newton-Raphson load distribution. Finally, by comparing the answers, the correctness



of the proposed method can be guaranteed. There are different ways to compare the answers obtained. The numerical values of the answers in the time domain can be compared. Other methods include comparing the probabilistic distribution function of the output variables and the selected model coefficients for the output data. Due to the possible nature of the AC load distribution problem, we receive different answers each time the output model is simulated. This can be explained by the randomly selected AC model noise component. However, to evaluate the accuracy of the proposed method, the data related to the random noise component used to simulate the active power and reactive input models can be used to simulate the output AC models in the proposed method. In other words, the components of random noise are considered in the same way in these two methods. The following figures show the point-to-point response values in the time domain for both AC and Newton-Raphson load distribution methods. As can be seen in the figures below, each simulation was performed for 100 time intervals. The continuous lines show the response of the Newton-Raphson method, and the circular lines show the shape of the response resulting from the proposed method.

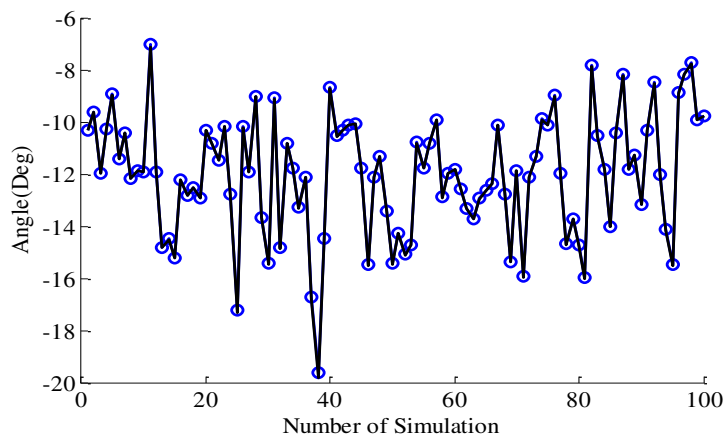


Figure 1: AC corresponding to bus angle No. 3 using parity of random noise values

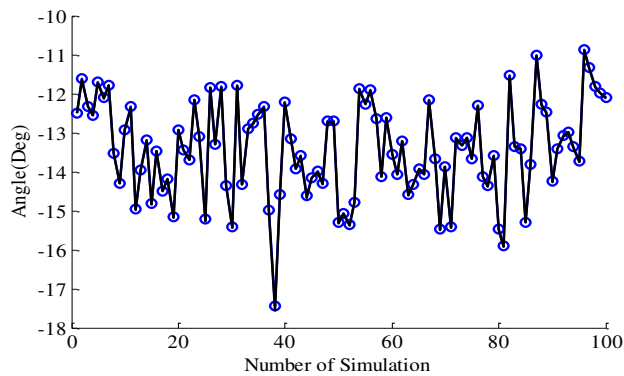


Figure 2: AC corresponding to bus angle No. 6 using parity of random noise values

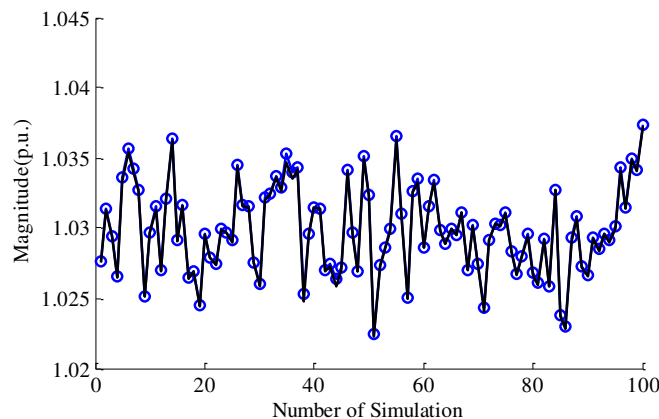


Figure 3: AC corresponding to bus voltage range No. 10 using parity of random noise values

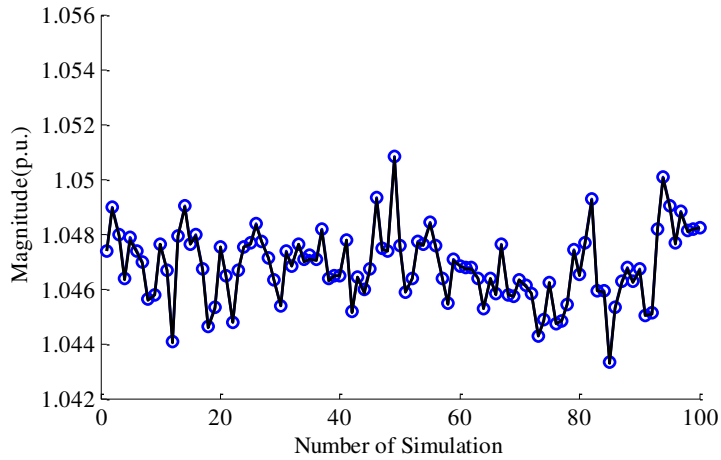


Figure 4: Ac related to bus voltage range 13 using parity of random noise values

The following figures show the probabilistic distribution function to compare the responses of the two methods. Each simulation was performed for 10,000 samples. An improved kernel method has been used to estimate the point-to-point data distribution function. In comparing the probabilistic distribution function of the responses, the random noise values are considered differently. Also, the continuous response line of the Newton-Raphson method and the dashed lines are the response of the proposed method.

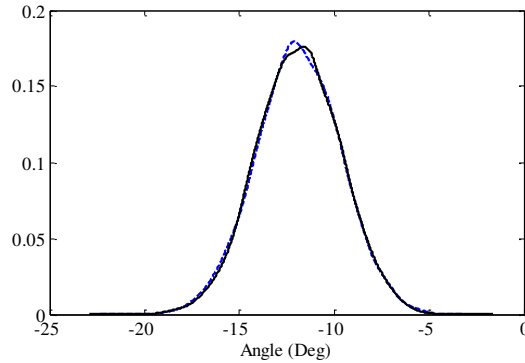


Figure 5: Probable bass angle distribution function number 3

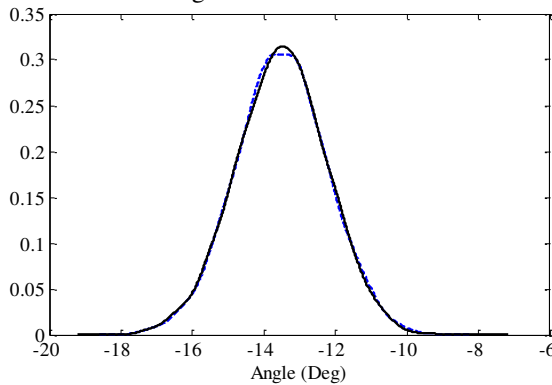


Figure 6: Probabilistic bus angle distribution function number 6

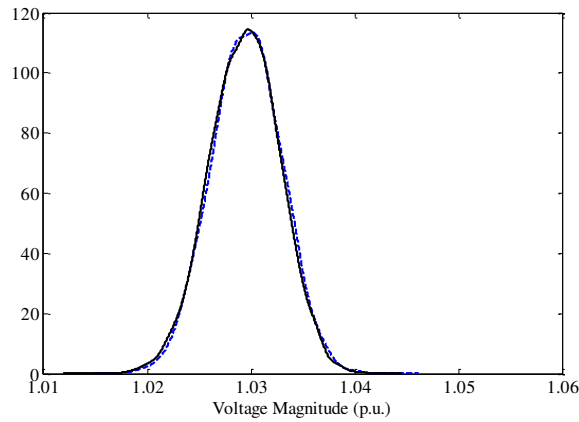


Figure 7: Probable distribution voltage range of bus voltage number 10

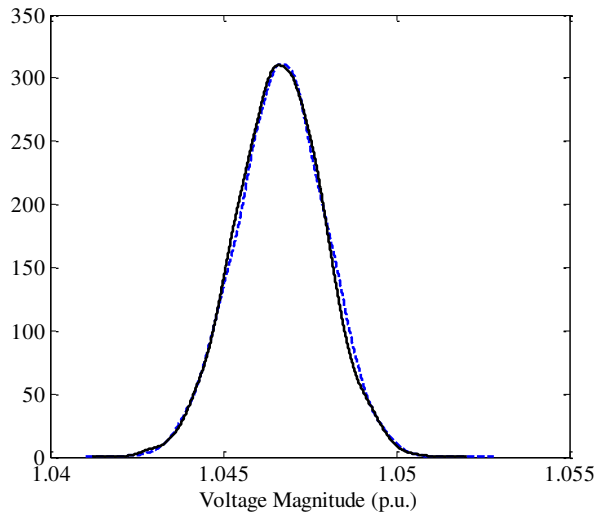


Figure 8: Probability distribution function of bus voltage range No. 13

The table below also shows the adapted AC model coefficients for the output AC model simulation data and the responses obtained from the proposed method. Here, the values for the random noise components are assumed to be the same for both methods.

Table 6: Comparison of model coefficients matched to the answers

Variables	Secondary coefficients		Initial coefficients	
	Newton-Raphson	AC	Newton-Raphson	AC
θ_3	0.339963	0.341461	0.0421778	0.0407418
θ_6	0.396185	0.398428	-0.029732	-0.031978
$ V_{10} $	0.426977	0.428088	-0.0730485	-0.0739606
$ V_{13} $	0.257789	0.260705	0.0342445	0.0320419



IV. RESULTS

The problem of network rearrangement in power systems

Rearranging or restructuring the network is one of the least expensive ways to reduce losses and increase the capacity of lines in the power network. Distribution networks in the power system are designed radially, but in order to increase the reliability of the subscribers, sometimes different power supply paths are considered for different loads in the network. Due to the variety of loads in the distribution system, including domestic, industrial and commercial loads, there are different types of load profiles in the network. Each of these loads will have different load profiles depending on different seasons, days of the week and different hours. The network is rearranged for various purposes such as reducing losses, improving the voltage profile in the network, balancing the load in the feeders and also due to improving some reliability indicators. Network restructuring is done by changing the status of existing switches on power system lines. So that by performing appropriate maneuvers, the percentage of network losses can be reduced. Load distribution calculations are required to calculate losses in the power grid. In distribution networks, where the problem of rearrangement is often raised, two general Newton-Raphson methods and the proposed load distribution algorithm are used. The Newton-Raphson load distribution method does not respond well to some networks at the distribution level and may lead to divergence. In power grid rearrangement methods, some system constraints must be considered so that the proposed topology can withstand the minimum network conditions. Different constraints apply to different issues, but the most important limitations that arise between almost all rearrangement issues include voltage, current, network radius, and power supply limitations for all system loads. The equations for the allowable voltage and current limits in the power system are shown below:

$$\begin{aligned} V^{min} &\leq |V_f^i| \leq V^{max} & f = 1, \dots, N_F & \quad i = 1, \dots, N_B \\ I^{min} &\leq |I_f^l| \leq I^{max} & f = 1, \dots, N_F & \quad l = 1, \dots, N_L \end{aligned}$$

In this equation N_F is the number of feeders, N_B is the number of buses and N_L is the number of branches or network lines. Similarly, in each step and by performing load distribution for each of the network topologies, the losses related to the dth day, in feeder f and line l can be calculated according to the following equation

$$Ploss_f^l(d) = R_f^l |I_f^l(d)|^2$$

The losses for the annual interval are then calculated from Equation 3.

$$Tloss = \sum_{d=1}^{365} \sum_{f=1}^{N_F} \sum_{l=1}^{N_L} Ploss_f^l(d)$$

Various methods have been proposed to solve the problem of rearrangement of the power network, which is one of the large and difficult issues. Extensive innovations have been made in the use of analytical and non-analytical methods in solving optimization problems bound to the restructuring of the power network. Finally, the purpose of solving the optimization problem is to minimize expression 4:

$$objective\ function = \min(Tloss)$$

Proposed algorithm

In this section, the proposed combined method, which is one of the non-analytical methods, is used to solve the optimization problem. This method is based on the formation of consecutive and appropriate populations from the problem answer space to the optimal answer. The proposed method uses operators based on the values of the objective function for each member to update the members of the population in a generation. If the ith member in this problem is represented by the vector $x_i = (x_{i1}, x_{i2}, \dots, x_{iD})$ will indicate the open or closed status of each switch, and D is the number of switches in the network. Also, according to the best values of the objective function obtained from previous generations for the i member, the status of the corresponding switches is stored in the variable $p_i = (p_{i1}, p_{i2}, \dots, p_{iD})$. The vector $v_i = (v_{i1}, v_{i2}, \dots, v_{iD})$ also indicates the rate of change or probability of change of status for each of the switches from one generation to the next, for the i member. Since the nature of the vector $v_i = (v_{i1}, v_{i2}, \dots, v_{iD})$ in binary mode can indicate the probability that the switches are one, a conversion function is used to limit the range of members of this vector to the range of zero and one. The Sigmoid function defined as $S(v_{id}^{new}) = \frac{1}{1+e^{-v_{id}^{old}}}$ is used to update the v_i vector. According to the index for the end of this algorithm, all the steps to create a new generation continue until the answer is reached. In BPSO algorithm, the constants c_1 and c_2 are the training coefficients and w is the inertia coefficient. The coefficient of inertia changes the boundaries of the response space, so that smaller coefficients tend to local responses and values of larger inertia coefficients tend to absolute optimal responses.



Proposed model in network rearrangement

In this chapter, the proposed model is used to model the system loads, which can consider the effect of synchronization of loads and the relationship between different loads in the system. In other words, instead of considering the annual load profile, the proposed models are used. In this section, it is assumed that the proposed model for each of the network loads can simulate the active power values on a daily basis over a year. Reactive power of system loads are also modeled as active loads. For model simplicity. Selected for modeling all times in the network. The aim of the optimization problem is to find the best network topology over a period of one year so that the sum of the average daily losses during the year has the lowest value for this network. The proposed method is also used in MATLAB software to solve the optimization problem. To solve this problem, in the proposed method, the status of network switches is changed in such a way that the radial nature of the studied network is maintained and also all network loads are fed and none of the loads are left without power supply. To apply the radial condition to the optimization method, all loops with N.O. switches must be applied. Form at least one of the switches is open. Also, for the correct condition of feeding all the network loads, except for the end loads of the feeders, the rest of the network loads must be connected to at least two lines whose switches are closed. Here, the proposed convective load distribution method is used to solve the AC load distribution problem in each iteration. At each stage of load distribution, the problem constraints that include the thermal allowance for the lines or the maximum flow through the lines must be checked. Also, the voltage regulation limit and the maximum and minimum allowable voltage must be observed separately. The constraints on the voltage and current limits are shown in Equation 1.

As mentioned in Chapter 3, since the AC load distribution method is based on the linearization of the proposed method, the load distribution equations must first be linearized around an average point. These average points are selected according to the model average. If all the inputs of this method are in the form of a model, the load distribution output will be the model, which includes an analytical model of the voltage range and angles of each of the network buses. Thus, if the input model in this method can simulate the loads of the sample system during a year and on a daily basis, the analytical output models will be able to simulate the voltage range and angles of the system buses during a year. Since in this case the goal is to find the losses related to a sample system during a year and for a specific network topology, this method can be used to solve the load distribution problem. Because according to the obtained model for each of the network topologies and performing numerical simulations for each of the voltage and bus angle variables, the current and then the network losses can be easily estimated.

The steps of rearranging the sample network and using the AC load distribution method are as follows:

- 1- Creating suitable models for active and reactive loads of the sample system and selecting constants related to the proposed method to solve the optimization problem.
- 2- Performing load distribution by Newton-Raphson method for the average input model for linearization of load distribution equations in the formulation method
- Selecting a random primary population for possible topologies in the sample system
- 4- Using the proposed algorithm to find the optimal switching status in the system
- 5- Checking the restrictions related to voltage and current limits in the load distribution problem
- 6- If the limit constraints are violated, the value of the objective function related to that member is not considered
- 7- Check the number of iterations to end the problem algorithm

Simulation results comparison

In this study, a 69-bus radial bus, which is an 11 kV distribution network, was selected for simulation. The study network is proposed. The appendix shows the 69-bus network topology and information about loads and lines. Each line is assumed to have a separate switch, so there are 79 switches in the network for the total number of lines. The 69-bus network has 11 switches that are normally open, and closing these switches creates loops in the network. So the other 68 switches on the network are normally closed. This network also has 4 main feeders that have different loads on each feeder. In these simulations, the constants in the proposed method, including the inertia coefficient w equal to one and the training coefficients c_1 and c_2 equal to 2, have been selected. The number of members in each generation and the number of repetitions or the number of generations in this issue are considered in two cases of 30 members and 40 members, as well as the number of 50 repetitions. The autoregressive coefficient in the model for simulating all active and reactive loads in the network is considered equal to 0.3. Also, the values of standard noise deviation related to each of the variables are selected as 0.1 of the model average. The average of the model is also selected according to the definite information, for the active and reactive loads that are available in the 69-bus network. Below is the status of the simulations for 30 members in each generation and 50 replicates. The annual loss rate for the standard network topology is 83.045 MW and for the network with the new topology in the proposed method is 74.498 MW. This



represents a 10.3% reduction in annual losses for the network. Also, the status of open or closed network switches before and after rearrangement.

The minimum and maximum voltage values during the year are 0.905 and 1 per unit for the standard network and 0.925 and 1 for the restructured network, respectively. Also, the simulation status of 40 members in each generation and 50 replications are checked below. In this case, the models are simulated separately and independently of the previous mode. The annual loss is 74,435 MW, which is a decrease of 10.4%, almost the same as before. The status of network switches is also shown in Table 1. The minimum and maximum voltage values for one year for the proposed network topology in this case are 0.927 and 1 per unit, respectively.

Check the correctness of the proposed method

In order to check the correctness of the proposed method, input simulation in the problem has been used. In this way, they are first numerically simulated over a period of one year. Then, using the AC load distribution method and considering the voltage and current constraints, the annual losses for the sample system are calculated. Finally, as in the first part of the problem, the proposed algorithm is used to find the optimal switching in the system. To test the simulations with 30 and 40 members, the above method has been used to find the optimal network response. In performing the simulations in this section, the noise values related to the simulations in the proposed method are used, but as mentioned above, the noise values are different for the 30 and 40 member modes. The annual network losses in these two cases are 73,793 and 74,435 MW, respectively, which shows a decrease of almost 10%. The following table shows the results related to the status of network switches in these two different modes.

Also, the minimum and maximum voltage values in the network buses are 0.931 and 1, respectively, in the case of 30 members, and 0.927 and 1, respectively, in the case of 40 members. According to the results, the values of the objective function are reduced appropriately, but the switching situation is not the same in these two methods. As in the first situation with 30 members, although the target function is reduced for both modes, the status of the switches is not the same throughout the network. But in the case of 40 members per generation, both methods have reached a single response and the same switches in the network have been selected to stay open. But the advantage of using the load distribution method is to perform less load distribution for each member and given topologies. In order to use the Newton-Raphson load distribution method, according to the number of members of each generation and the number of iterations of the problem, it will be necessary to perform a large number (365 members of each generation, the number of iterations) to solve the problem. While using the load distribution method, we will need a smaller number (number of members per generation, number of repetitions) of load distribution and (number of members per generation, number of repetitions) load, Newton-Raphson load distribution will be used. Therefore, due to the fact that load distribution provides an annual analytical model of system variables, we will not need to perform load distribution for each day in a year. However, according to the linearization in the load distribution method, if the input data deviates from the mean values used to linearize the equations, the amount of computational error can affect the results. To compare the execution time of Newton-Raphson load distribution and AC load distribution in this method, 40 members and 80 repetitions are considered. This case is checked for two time intervals of 365 days and 1000 days and the time related to the implementation of each is given in the table below.

Table 9: Comparison of execution times of load distribution methods in the problem of power network restructuring

Model	Program execution time in minutes
Newton-Raphson load distribution (365 days)	82.1
Load playback (365 days)	67.6
Newton-Raphson load distribution (1000 days) Load playback	213
Load playback (1000 days)	98.44

V. CONCLUSION

The purpose of this paper is to focus on the use of analytical and numerical models in the power system. Because due to changes in load and production in the power system and in the time domain, modeling these variables in the time domain will be appropriate. Now, if these modeling are done properly, they can simulate the relationship between different variables in the power system. As we know, one of the main topics in power system load distribution studies is to consider the relationship between input variables in the problem. On the other hand, due to the dependence of



output mode variables including voltage and phase amplitude, multivariate models need to be used to model these variables. In this paper, AC input models have been used directly in load distribution studies, so that the output is an analytical and multivariate model of amplitude and voltage phase. In order to perform load distribution, linearized equations have been used in the proposed method. In the fourth chapter, the load distribution introduced in this paper is used to perform rearrangement at the level of a distribution network. One of the advantages of using AC load distribution method in this issue is reducing the number of definite load distributions. Network rearrangement issues expand as the network size increases. So that the need to play consecutive loads is felt. In this chapter, the problem of distribution network restructuring is solved by using load distribution and the answers are compared correctly with a definite method. Existence of parameters with discrete values in the power system requires proper modeling in the time domain and by models. Some of these variables include the location of the pulse transformer, the output power of the CHP dispersed production units, and the capacitive banks. Existing models can not properly simulate these variables. The models used so far to simulate discrete variables are mostly based on discrete Markov models. One of the disadvantages of this method is the increase in the number of unknown parameters with increasing problem size. Therefore, the need for an alternative model in this area is felt. The model used in this paper, according to the modeling steps of this method, simulations must be performed for a long period of time. Because if these models are simulated in a relatively short period of time, the mismatch of the simulated data density function will be significant.

Appendix

IEEE 14-bus network information

The following tables show the 14-bus network data used in this paper.

Table: 14 bus network data

Busbar		Voltage p.u.	Active power (MW)		Load Reactive power (MVar)
Number	Type		Generation	Load	
1	Slack	1.06	----	----	----
2	PV	1.045	40.04	21.74	12.7
3	PV	1.01	----	94.2	19
4	PQ	----	----	47.8	-3.9
5	PQ	----	----	7.6	1.6
6	PV	1.07	----	11.2	7.5
7	PQ	----	----	----	----
8	PV	----	15	----	----
9	PQ	----	----	29.5	16.6
10	PQ	----	----	9	5.8
11	PQ	----	----	3.5	1.8
12	PQ	----	----	6.1	1.6
13	PQ	----	----	13.5	5.8
14	PQ	----	----	14.9	5

Table: Data for 14 bus lines

Busbar		Resistance p.u.	Reactance p.u.	Susceptance p.u.	Transformer Tap (%)
Sending	Receiving				
1	2	0.01938	0.05917	0.02640	----
1	5	0.05403	0.22304	0.02640	----
2	3	0.04699	0.19797	0.02190	----
2	4	0.05811	0.17632	0.01870	----
2	5	0.05695	0.17388	0.01700	----
3	4	0.06701	0.17103	0.01730	----
4	5	0.01335	0.04211	0.00640	----
4	7	----	0.20912	----	----



4	9	----	0.55618	----	----
5	6	----	0.25202	----	----
6	11	0.09498	0.19890	----	----
6	12	0.12291	0.25581	----	----
6	13	0.06615	0.13027	----	----
7	8	----	0.17615	----	----
7	9	----	0.11001	----	----
9	10	0.03181	0.08450	----	----
9	14	0.12711	0.27038	----	----
10	11	0.08205	0.19207	----	----
12	13	0.22092	0.19988	----	----
13	14	0.17093	0.34802	----	----
9	9	----	-5.26000	----	----

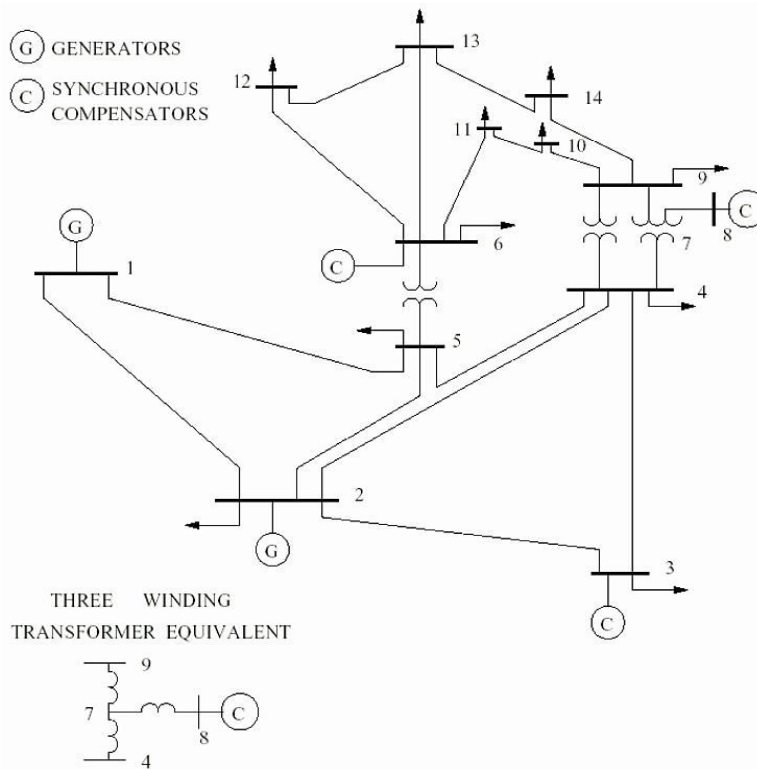


Figure: IEEE standard 14-bus single-line network display

69 bus network information

The table of load and line information for the 69-bus network and the topology of this network is given below. Also, the values of the allowable current passing through the lines and the minimum and maximum voltage in different bus buses are given below.

Table: Information on loads and lines in the 69-bus network

Branch number	Elementary bass number	End bass number	Resistance (ohm)	Inductance (ohm)	Active power (kW)	Reactive power (kW)
1	1	2	1.097	1.074	100	90
2	2	3	1.463	1.432	60	40
3	3	4	0.731	0.716	150	130



4	4	5	0.366	0.358	75	50
5	5	6	1.828	1.79	15	9
6	6	7	1.097	1.074	18	14
7	7	8	0.731	0.716	13	10
8	8	9	0.731	0.716	16	11
9	4	10	1.08	0.734	20	10
10	10	11	1.62	1.101	16	9
11	11	12	1.08	0.734	50	40
12	12	13	1.35	0.917	105	90
13	13	14	0.81	0.55	25	15
14	14	15	1.944	1.321	40	25
15	7	68	1.08	0.734	100	60
16	68	69	1.62	1.101	40	30
17	1	16	1.097	1.074	60	30
18	16	17	0.366	0.358	40	25
19	17	18	1.463	1.432	15	9
20	18	19	0.914	0.895	13	7
21	19	20	0.804	0.787	30	20
22	20	21	1.133	1.11	90	50
23	21	22	0.475	0.465	50	30
24	17	23	2.214	1.505	60	40
25	23	24	1.62	1.11	100	80
26	24	25	1.08	0.734	80	65
27	25	26	0.54	0.367	100	60
28	26	27	0.54	0.367	100	55
29	27	28	1.08	0.734	120	70
30	28	29	1.08	0.734	105	70
31	1	30	0.366	0.358	80	50
32	30	31	0.731	0.716	60	40
33	31	32	0.731	0.716	13	8
34	32	33	0.804	0.787	16	9
35	33	34	1.17	1.145	50	30
36	34	35	0.768	0.752	40	28
37	35	36	0.731	0.716	60	40
38	36	37	1.097	1.074	40	30
39	37	38	1.463	1.432	30	25
40	32	39	1.08	0.734	150	100
41	39	40	0.54	0.367	60	35
42	40	41	1.08	0.734	120	70
43	41	42	1.836	1.248	90	60
44	42	43	1.296	0.881	18	10
45	40	44	1.188	0.807	16	10



46	44	45	0.54	0.367	100	50
47	42	46	1.08	0.734	60	40
48	35	47	0.54	0.367	90	70
49	47	48	1.08	0.734	85	55
50	48	49	1.08	0.734	100	70
51	49	50	1.08	0.734	140	90
52	1	51	0.366	0.358	60	40
53	51	52	1.463	1.432	20	11
54	52	53	1.463	1.432	40	30
55	53	54	0.914	0.895	36	24
56	54	55	1.097	1.074	30	20
57	55	56	1.097	1.074	43	30
58	52	57	0.27	0.183	80	50
59	57	58	0.27	0.183	240	120
60	58	59	0.81	0.55	125	110
61	59	60	1.296	0.881	25	10
62	55	61	1.188	0.807	10	5
63	61	62	1.188	0.807	150	130
64	62	63	0.81	0.55	50	30
65	63	64	1.62	1.101	30	20
66	62	65	1.08	0.734	130	120
67	65	66	0.54	0.367	150	130
68	66	67	1.08	0.734	25	15
69	9	50	0.908	0.726	-----	-----
70	9	38	0.381	0.244	-----	-----
71	15	46	0.681	0.544	-----	-----
72	22	67	0.254	0.203	-----	-----
73	29	64	0.254	0.203	-----	-----
74	45	60	0.254	0.203	-----	-----
75	43	38	0.454	0.363	-----	-----
76	39	59	0.454	0.363	-----	-----
77	21	27	0.454	0.363	-----	-----
78	15	9	0.681	0.544	-----	-----
79	67	15	0.454	0.363	-----	-----

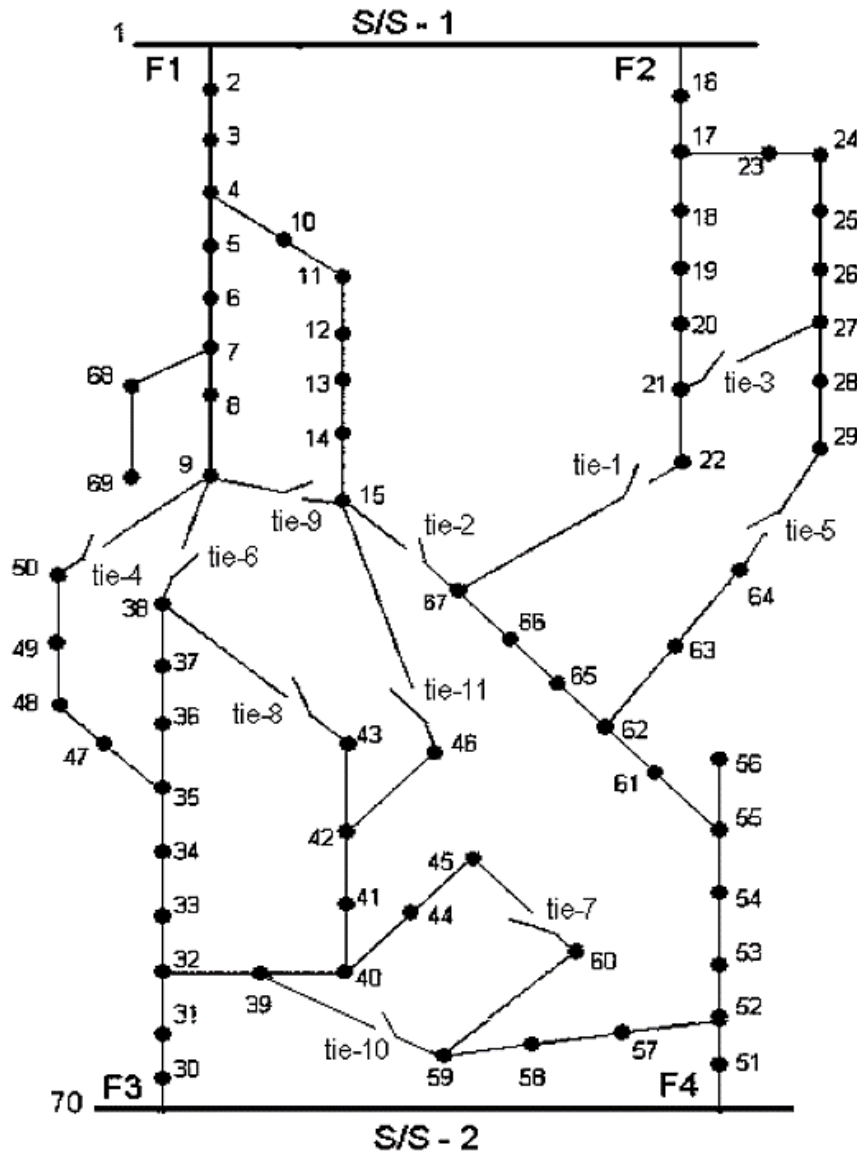


Figure: 69-bus network

The minimum and maximum allowable voltage values in each of the 69-bus network buses are 0.85 and 1.05 per unite, respectively. Also allowed current of branches 1 to 8, 270 amps, branches 9 to 16, 208 amps, branches 17 to 23, 270 amps, branches 24 to 30, 208 amps, branches 31 to 39, 270 amps, branches 40 to 51, 208 amps, branches 52 to 57, 270 amps, branches 58 to 68, 208 amps and branches 69 to 79, 234 amps.

REFERENCES

[1] Masoud Farivar, Christopher R. Clarke, Steven H. Low, and K. Mani Chandy. Inverter var control for distribution systems with renewables. In Proceedings of IEEE SmartGridComm Conference, October 2011.
 [2] J. Lavaei and S. H. Low. Zero duality gap in optimal power flow problem. IEEE Trans. on Power Systems, 27(1):92–107, February 2012. [50] S. Bose, D. Gayme, S. H. Low, and K. M. Chandy. Optimal power flow over tree networks. In Proc. Allerton Conf. on Comm., Ctrl. and Computing, October 2011.
 [3] Florin Capitanescu, “Critical review of recent advances and further developments needed in AC optimal power flow”, Electric Power Systems Research, vol. 136, pp. 57–68, July 2016.
 [4] Florin Capitanescu and Louis Wehenkel, “Experiments with the interiorpoint method for solving large scale Optimal Power Flow problems”, Electric Power Systems Research, vol. 95, pp. 276–283, Feb. 2013.



- [5] Anya Castillo and R. O'Neill, "Computational Performance of Solution Techniques Applied to the ACOFP", Tech. Rep., 2013.
- [6] B. Stott and O. Alsac, "Optimal power flow: Basic requirements for real-life problems and their solutions", 2012.
- [7] B. Stott, J. Jardim, and O. Alsac, "DC Power Flow Revisited", IEEE Transactions on Power Systems, vol. 24, no. 3, pp. 1290–1300, Aug. 2009.
- [8] J. A. Momoh and J. Z. Zhu, "Improved interior point method for OPF problems", IEEE Transactions on Power Systems, vol. 14, no. 3, pp. 1114–1120, Aug. 1999.
- [9] A. L. Motto, F. D. Galiana, A. J. Conejo, and J. M. Arroyo, "Networkconstrained multiperiod auction for a pool-based electricity market", IEEE Transactions on Power Systems, vol. 17, no. 3, pp. 646–653, Aug. 2002.
- [10] T.J. Overbye, Xu Cheng, and Yan Sun, "A comparison of the AC and DC power flow models for LMP calculations", in Proceedings of the 37th Annual Hawaii International Conference on System Sciences, 2004.
- [11] K. Purchala, L. Meeus, D. Van Dommelen, and R. Belmans, "Usefulness of DC power flow for active power flow analysis", in IEEE PES General Meeting, 2005, June 2005, pp. 454–459 Vol. 1.
- [12] R. Madani, S. Sojoudi, and J. Lavaei, "Convex Relaxation for Optimal Power Flow Problem: Mesh Networks", IEEE Transactions on Power Systems, vol. 30, no. 1, pp. 199–211, Jan. 2015.
- [13] Masoud Farivar and Steven H. Low, "Branch Flow Model: Relaxations and Convexification—Part I", IEEE Transactions on Power Systems, vol. 28, no. 3, pp. 2554–2564, Aug. 2013.
- [14] Carleton Coffrin, Hassan L. Hijazi, and Pascal Van Hentenryck, "The QC Relaxation: A Theoretical and Computational Study on Optimal Power Flow", IEEE Transactions on Power Systems, vol. 31, no. 4, pp. 3008–3018, July 2016.
- [15] Javad Lavaei and Steven H. Low, "Zero Duality Gap in Optimal Power Flow Problem", IEEE Transactions on Power Systems, vol. 27, no. 1, pp. 92–107, Feb. 2012.
- [16] M. Nick, R. Cherkaoui, J. Y. LeBoudec, and M. Paolone, "An Exact Convex Formulation of the Optimal Power Flow in Radial Distribution Networks Including Transverse Components", IEEE Transactions on Automatic Control, vol. PP, no. 99, pp. 1–1, 2017.
- [17] C. Chen, A. Atamturk, and S. S. Oren, "Bound Tightening for the Alternating Current Optimal Power Flow Problem", IEEE Transactions on Power Systems, vol. 31, no. 5, pp. 3729–3736, Sept. 2016. [18] Carleton Coffrin, Hassan L. Hijazi, and Pascal Van Hentenryck, "Strengthening Convex Relaxations with Bound Tightening for Power Network Optimization", in Principles and Practice of Constraint Programming. Aug. 2015, Lecture Notes in Computer Science, pp. 39–57, Springer, Cham.
- [19] C. Coffrin, H. L. Hijazi, and P. Van Hentenryck, "Strengthening the SDP Relaxation of AC Power Flows With Convex Envelopes, Bound Tightening, and Valid Inequalities", IEEE Transactions on Power Systems, vol. 32, no. 5, pp. 3549–3558, Sept. 2017.
- [20] B. Kocuk, S. S. Dey, and X. A. Sun, "Inexactness of SDP Relaxation and Valid Inequalities for Optimal Power Flow", IEEE Transactions on Power Systems, vol. 31, no. 1, pp. 642–651, Jan. 2016.
- [21] Garth P. McCormick, "Computability of global solutions to factorable nonconvex programs: Part I — Convex underestimating problems", Mathematical Programming, vol. 10, no. 1, pp. 147–175, Dec. 1976. [22] Ksenia Bestuzheva, Hassan Hijazi, and Carleton Coffrin, "Convex Relaxations for Quadratic On/Off Constraints and Applications to Optimal Transmission Switching", 2019.
- [23] D. Shchetinin, T. Tinoco De Rubira, and G. Hug, "On the Construction of Linear Approximations of Line Flow Constraints for AC Optimal Power Flow", IEEE Transactions on Power Systems, 2018.
- [24] Dmitry Shchetinin, Optimization of Power System Operation: Approximations, Relaxations, and Decomposition, Doctoral Thesis, ETH Zurich, Dec. 2018.
- [25] R. D. Zimmerman, C. E. Murillo-Sanchez, and R. J. Thomas, "MATPOWER: Steady-State Operations, Planning, and Analysis Tools for Power Systems Research and Education", IEEE Transactions on Power Systems, vol. 26, no. 1, pp. 12–19, Feb. 2011.
- [26] Timothy A. Davis and Ekanathan Palamadai Natarajan, "Algorithm 907: KLU, A Direct Sparse Solver for Circuit Simulation Problems", ACM Trans. Math. Softw., vol. 37, no. 3, pp. 36:1–36:17, Sept. 2010.



**Impact Factor:
7.569**



INTERNATIONAL JOURNAL OF INNOVATIVE RESEARCH

IN SCIENCE | ENGINEERING | TECHNOLOGY

 9940 572 462  6381 907 438  ijirset@gmail.com



www.ijirset.com

Scan to save the contact details